Letter Vol. 43, No. 23 / 1 December 2018 / Optics Letters 5741

Strong magnetochiral dichroism in chiral/magnetic layered heterostructures

Aristi Christofi

National and Kapodistrian University of Athens, Department of Physics, Section of Solid State Physics, Panepistimioupolis, GR-157 84 Athens, Greece (aristi.christofi@gmail.com)

Received 17 October 2018; revised 2 November 2018; accepted 6 November 2018; posted 7 November 2018 (Doc. ID 348518); published 21 November 2018

In this Letter, we propose a nonreciprocal heterostructure which combines magnetism and chirality in a simple, easy-to-fabricate design and exhibits at least two orders of magnitude larger magnetochiral dichroism, compared to other proposed metamaterials. This effect stems from the simultaneous lack of time-reversal and space-inversion symmetries and is enhanced by collective slow-photon modes originating from the strong bending of the photonic bands at the Brillouin zone boundaries. We investigate the optical properties of this bianisotropic multilayer heterostructure, consisting of consecutive bilayers of chiral and magnetic materials, embedded in air, and discuss the associated photonic band structure and transmission/absorption spectra obtained by means of full electrodynamic calculations.

https://doi.org/10.1364/OL.43.005741

Nonreciprocal photonic structures which lack both space-inversion and time-reversal symmetries have been of great interest in recent years for multiple reasons, for example, designing technologically important devices such as circulators and isolators [1]. More specifically, spectral nonreciprocity, a really interesting property in photonics, can be caused by systems which combine this absence of space-inversion and time-reversal symmetries [2] at the same time, and various magnetophotonic architectures without an inversion center have been proposed for this purpose [3–6].

The breaking of time-reversal symmetry can be accomplished with magneto-optical effects driven by external or internal magnetic fields, while layered composites provide a versatile platform for realizing asymmetric heterostructures. Structural (due to a chiral arrangement of constituents) and molecular (due to inherent chiral structure of the molecules themselves) chirality also removes space-inversion symmetry, and composite designs with such chiral components were found to possess sizable omnidirectional photonic bandgaps [7,8], as well as partial bandgaps for just one of the two circular polarizations [9,10] that can give rise to strong circular dichroism [11–13].

Magnetochiral anisotropy effects have long been anticipated theoretically, either in refraction (birefringence) or in absorption/emission (dichroism) [14–20]. These effects are clearly nonreciprocal, stemming from the simultaneous lack of time-reversal and space-inversion symmetries in a magnetized chiral material and should be identified as different from their reciprocal counterparts, which are induced solely by either chirality or magnetism. Magnetochiral anisotropy, is of great interest for a variety of reasons. It has been proposed as a possible explanation for the homochirality of life [21] and may be important in the context of fundamental interactions between light and matter.

In this Letter, we report on the optical response of a nonreciprocal bianisotropic multilayer heterostructure, consisting of consecutive bilayers of chiral and magnetic materials. We combine magnetism and chirality in a simple, easy-to-fabricate design and investigate an important nonreciprocal effect, magnetochiral dichroism resulting from the combination of optical activity in chiral systems and magnetically induced optical activity. Our results reveal that the proposed metamaterial exhibits at least a two orders of magnitude larger magnetochiral dichroism, compared to other proposed nanostructures.

To investigate the optical properties of such a composite structure, we developed a versatile six-vector formalism in order to calculate the eigenmodes of the electromagnetic (EM) field in a homogeneous bianisotropic medium, as well as the transmission, reflection, and absorption coefficients to finally obtain the associated photonic band structure and transmission spectra. In our analysis, we solve Maxwell equations taking into account the following phenomenological constitutive relations, which describe the response of general bianisotropic materials to EM fields:

$$\begin{pmatrix} \frac{1}{\epsilon_0}\mathbf{D} \\ \frac{1}{\sqrt{\epsilon_0\mu_0}}\mathbf{B} \end{pmatrix} = \begin{pmatrix} \epsilon & \boldsymbol{\xi} \\ \boldsymbol{\zeta} & \boldsymbol{\mu} \end{pmatrix} \begin{pmatrix} \mathbf{E} \\ \sqrt{\frac{\mu_0}{\epsilon_0}}\mathbf{H} \end{pmatrix}, \tag{1}$$

where $\mathbf{E}$ (in V/m) and $\mathbf{H}$ (in A/m) are the electric and magnetic fields, and $\mathbf{D}$ (in $\mathrm{C/m^2}$) and $\mathbf{B}$ (in $\mathrm{Wb/m^2}$) are the electric and magnetic flux densities, respectively. The vacuum electric permittivity and magnetic permeability are ϵ_0 and μ_0, respectively. The relative electric permittivity ϵ, magnetic permeability $\boldsymbol{\mu}$, and magnetoelectric cross-coupling $\boldsymbol{\xi}$ and $\boldsymbol{\zeta}$ are 3×3 tensors, with the latter being nonzero, e.g., for optically active chiral media. A detailed analysis of our methodology, which goes

beyond existing approaches that involve cumbersome nonlinear eigenvalue problems, is given in our recent publication [22].

The structure under study is a multilayer heterostructure consisting of consecutive bilayers of chiral and magnetic materials, magnetized along the growth direction which is assumed to be along the z axis. A schematic view of the bilayer is shown in the inset of Fig. 1, with a being the periodicity of the structure. The chiral and magnetic layers are of thicknesses $2a/3$ and $a/3$, respectively. The combination of chiral and magnetic materials provides the breaking of space-inversion symmetry through the chiral layer, while time-reversal symmetry is removed by the presence of the magnetic field. The proposed structure can be fabricated, e.g., by the combination of sputtering and chemical methods.

For the isotropic host medium, the 6×6 matrix of Eq. (1) is composed of these elements: $\epsilon_{ij} = \epsilon_h \delta_{ij}$ and $\boldsymbol{\mu}_{ij} = \mu_h \delta_{ij}$, while tensors $\boldsymbol{\xi}$ and $\boldsymbol{\zeta}$ are zero. For the case under study, the host medium is chosen to be air with $\epsilon_h = 1$ and $\mu_h = 1$. For the chiral medium, $\epsilon_{ij} = \epsilon_c \delta_{ij}$ and $\boldsymbol{\mu}_{ij} = \mu_c \delta_{ij}$, with $\epsilon_c = 2$ and $\mu_c = 1$. The magnetoelectric cross-coupling tensors are given by $\boldsymbol{\xi}_{ij} = i\gamma_c \delta_{ij}$ and $\boldsymbol{\zeta}_{ij} = -i\gamma_c \delta_{ij}$, where $\gamma_c = 0.01$. For the magnetic medium, the relative electric permittivity tensor, ϵ, at optical and infrared frequencies, has the form

$$\epsilon = \begin{pmatrix} \epsilon_m & -ig_m & 0 \\ ig_m & \epsilon_m & 0 \\ 0 & 0 & \epsilon_m \end{pmatrix}, \tag{2}$$

if the magnetization is along the z axis, with $\epsilon_m = 5$ and $g_m = 0.05$. The magnetic permeability $\boldsymbol{\mu}_{ij} = \mu_m \delta_{ij}$ with $\mu_m = 1$, while tensors $\boldsymbol{\xi}$ and $\boldsymbol{\zeta}$ are zero. The values for the magnetic material are realistic if we use magnetic garnets [23–25] and, for the chiral material, the assumed values of the chirality parameter, γ_c, can be achieved with substances such as poly-L-lactic acid, at free-space wavelengths around 632.8 nm [26].

In Fig. 1, we depict the photonic band structure of the heterostructure under study along the magnetization direction,

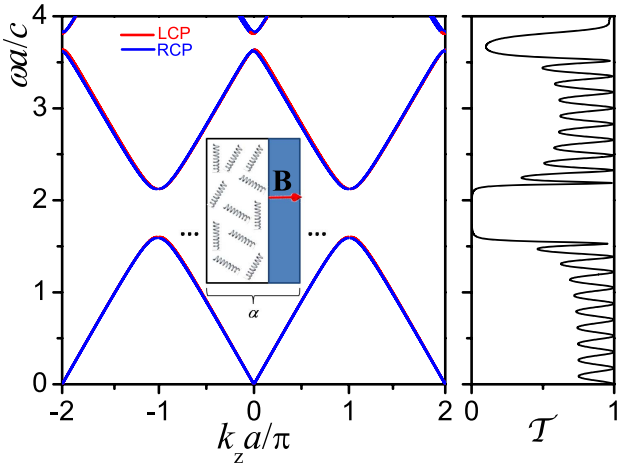

Fig. 1. Left-handed diagram: photonic band structure of the binary multilayer heterostructure under study, along the magnetization direction. A slab of the nanocomposite under study is shown in the inset. Right-handed diagram: corresponding transmission spectrum of a finite slab of thickness $d = 23a$, in air, magnetized perpendicular to its surfaces, for linearly polarized light incident in the direction of magnetization.

together with the corresponding transmission spectrum of a finite slab of it, magnetized perpendicular to its surfaces, for linearly polarized light incident in the direction of magnetization. In any bianisotropic medium, along any direction, the dispersion relation has two extended branches corresponding to the two linearly independent transverse polarization eigenmodes of the propagating waves. For the structure under study in which we have consecutive layers of materials with different refractive indices, we expect the opening of photonic bandgaps. In the left-handed diagram of Fig. 1, one can see the formation of a photonic bandgap, as a result of the destructive interference of the EM waves due to the periodic variation of the refractive index.

The corresponding transmittance of a finite slab of the given structure vanishes over the range of the photonic bandgap and exhibits Fabry–Perot oscillations outside the gap due to multiple reflections at the surfaces of the slab, as can be seen in the right-handed diagram of Fig. 1.

The modes of the EM field propagating along the z direction in this structure, the bilayer of which consists a chiral and a magnetic material, have the symmetry of the irreducible representations of the C_∞ continuous point group that consists of all proper rotations around the z axis and leaves this direction invariant [27]. Since C_∞ is an Abelian group (it is isomorphic to the SO(2) group), all of its irreducible representations are one-dimensional, thus implying that all bands must be nondegenerate. In our case, the bands correspond to the modes of right circular polarization (RCP) and left circular polarization (LCP)- [28]. This means that only light of the same circular polarization, incident normally on a slab of the given structure magnetized perpendicular to its surfaces, can excite the RCP and LCP bands, as shown in the middle and lower diagrams of Fig. 2. Moreover, the periodicity implies that

$$\omega_p(k_z + n2\pi/a) = \omega_p(k_z), \tag{3}$$

while, due to the simultaneous lack of time-reversal and space-inversion symmetries,

$$\omega_p(-k_z) \neq \omega_p(k_z), \tag{4}$$

with $n = 0, \pm 1, \pm 2, \ldots$ being the band index and $p =$ LCP, RCP.

The separation between the LCP and RCP dispersion curves and the nonreciprocal characteristics of the band diagram are not clearly observed in the scale of Fig. 1 but, in the top diagram of Fig. 2, the separation is clearly manifested as we focus at the region below the lower photonic bandgap at the top of the photonic bands. At the Brillouin zone boundaries, we have the formation of slow-photon modes that originate from the strong bending of the photonic bands. In the middle and lower diagrams of Fig. 2, we show the transmission and absorption spectra, respectively, for LCP and RCP light, incident normally, on a finite slab of the structure in the direction of magnetization. We take into account absorptive losses assuming $\epsilon_m = 5 + i0.0001$, $\mu_m = 1$, $g_m = 0.05$, $\epsilon_c = 2 + i0.002$, $\mu_c = 1 + i0.0005$, $\gamma_c = 0.01 + i0.001$, $\epsilon_h = 1$, and $\mu_h = 1$. These values are realistic and consistent with experimental data for optical frequencies [29,30], and they fulfill the restrictions required for a dissipative medium. We recall that for a biisotropic medium the following conditions have to be satisfied $\mathrm{Im}\epsilon_c \geq 0$, $\mathrm{Im}\mu_c \geq 0$, and $\mathrm{Im}\epsilon_c \mathrm{Im}\mu_c \geq (\mathrm{Im}\gamma_c)^2$, in order to have losses and not gain. For the same reason, restrictions apply

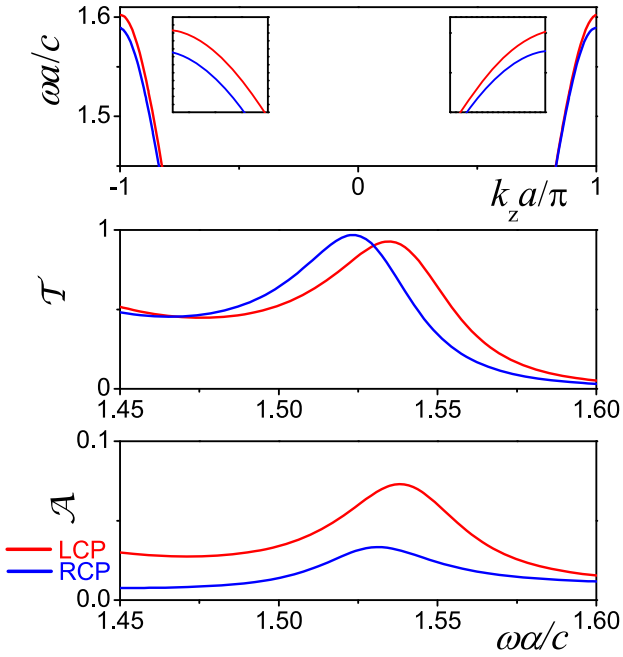

Fig. 2. Top diagram: an enlarged view of the dispersion diagram of Fig. 1 below the lower bandgap, in the band region of interest. Middle and lower diagrams: corresponding transmission (middle diagram) and absorption (lower diagram) spectra of a finite slab of thickness $d = 23a$, in air, magnetized perpendicular to its surfaces, for the left and right circularly polarized light incident in the direction of magnetization.

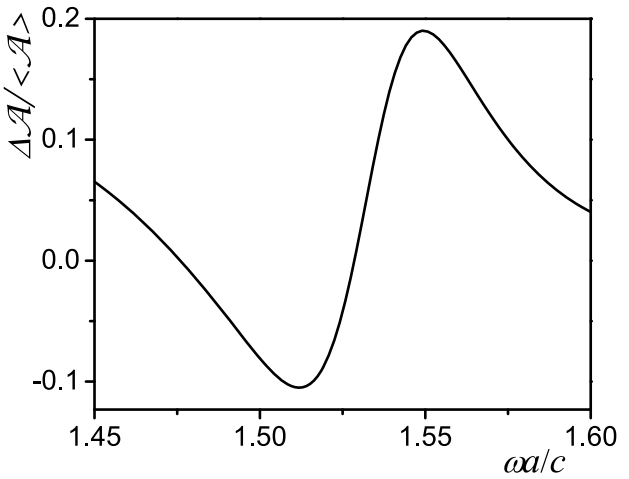

Fig. 3. Magnetochiral dichroism of a slab of the heterostructure under study, of thickness $d = 23a$, magnetized perpendicular to its surfaces, at normal incidence, in the region of the lowest-frequency band. Absorptive losses are taken into account.

for the case of a magnetic medium as well: $\mathrm{Im}\epsilon_m \geq 0$, $\mathrm{Im}\mu_m \geq 0$, and $-\mathrm{Im}\epsilon_m \leq \mathrm{Im}g_m \leq \mathrm{Im}\epsilon_m$.

As we can see from the spectra, absorption resonances follow transmission picks; therefore, when the modes have long lifetimes, they manage to get absorbed and, as a result, in these frequency regions, we expect the occurrence of strong nonreciprocal absorption effects.

The spectral region around the lower bandgap, shown in the diagrams of Fig. 2, is our region of interest on which we will focus and investigate a nonreciprocal absorption effect, magnetochiral dichroism. Magnetochiral dichroism is a nonreciprocal effect observed in magnetized chiral systems featuring an unbalanced absorption of unpolarized light depending on the direction of magnetization. As a quantitative measure of magnetochiral dichroism, we adopt the normalized anisotropy factor $\Delta\mathcal{A}/\langle\mathcal{A}\rangle$ [31], with $\Delta\mathcal{A} \equiv \mathcal{A}_+ - \mathcal{A}_-$ and $\langle\mathcal{A}\rangle \equiv (\mathcal{A}_+ + \mathcal{A}_-)/2$, where $\mathcal{A}_{+(-)}$ is the absorbance of unpolarized light incident on a slab of the structure in (opposite to) the direction of magnetization. We note that unpolarized light can be regarded as an incoherent superposition of LCP and RCP or, in general, of any two orthonormal polarization light modes. In order to study this effect we take into account absorptive losses, as previously. As can be seen in Fig. 3, strong magnetochiral diachroism, which corresponds to values of the normalized anisotropy factor as large as 0.2, is obtained near the top of the bands of Fig. 2, where the effect is enhanced by collective slow-photon modes which originate from the strong bending of the photonic bands at the Brillouin zone boundaries.

The obtained value of magnetochiral dichroism is considerably larger compared to other proposed metamaterials. At optical frequencies, a slab of magnetic garnet spheres in helical arrangement in a low-refractive-index nonmagnetic host material, three times thicker than the one considered here, exhibits a normalized anisotropy factor of about 0.1, which is two times smaller than the value we achieve in this Letter [32]. Moreover, compared to slabs of magnetoplasmonic helices of magnetite nanoparticles in solution [33] and of metal-coated magnetic nanoparticles in an optically active material [22], both 20 times thinner than the one considered here, we obtain a 50 times stronger effect.

From the above, it becomes clear that the novelty in this Letter relies on the fact that the proposed design gives stronger megnetochiral dichroism and, in addition, its fabrication is easier compared to the other metamaterials reported so far. It is worth noting that the structure under consideration was selected after proper optimization in order to obtain an enhanced effect. Therefore, this Letter opens up the way to the design of nanostructures with stronger magnetochiral anisotropy, which may find practical applications in miniaturized nonreciprocal photonic devices, as well as allowing polarization-independent control of slab absorption properties through magnetic field modulation.

In summary, we proposed a nonreciprocal bianisotropic multilayer heterostructure, consisting of consecutive bilayers of chiral and magnetic materials. We analyzed and discussed the associated photonic band structure diagrams, along with the corresponding transmission and absorption spectra. The proposed structure exhibits at least a two orders of magnitude larger magnetochiral dichroism compared to other proposed metamaterials, which stems from the simultaneous lack of time-reversal and space-inversion symmetries and is enhanced by collective slow-photon modes which originate from the strong band bending at the Brillouin zone boundaries.

Funding. "Strengthening Post Doctoral Research," State Scholarships Foundation (IKY) (2016-050-0503-7197).

Acknowledgment. A. Christofi acknowledges support by the Greek State Scholarships Foundation (IKY) through the program "Strengthening Post Doctoral Research."

REFERENCES

1. S. Fan, R. Baets, A. Petrov, Z. Yu, J. D. Joannopoulos, W. Freude, A. Melloni, M. Popović, M. Vanwolleghem, D. Jalas, M. Eich, M. Krause, H. Renner, E. Brinkmeyer, and C. R. Doerr, Science **335**, 38 (2012).
2. A. Figotin and I. Vitebsky, Phys. Rev. E **63**, 066609 (2001).
3. Z. Yu, G. Veronis, Z. Wang, and S. Fan, Phys. Rev. Lett. **100**, 023902 (2008).
4. Y. Hadad and B. Z. Steinberg, Phys. Rev. Lett. **105**, 233904 (2010).
5. A. B. Khanikaev, S. H. Mousavi, G. Shvets, and Y. S. Kivshar, Phys. Rev. Lett. **105**, 126804 (2010).
6. A. Christofi and N. Stefanou, Int. J. Mod. Phys. B **28**, 1441012 (2014).
7. A. Chutinan and S. Noda, Phys. Rev. B **57**, R2006 (1998).
8. O. Toader and S. John, Science **292**, 1133 (2001).
9. J. Lee and C. Chan, Opt. Express **13**, 8083 (2005).
10. M. Thiel, M. Decker, M. Deubel, M. Wegener, S. Linden, and G. von Freymann, Adv. Mater. **19**, 207 (2007).
11. P. C. P. Hrudey, B. Szeto, and M. J. Brett, Appl. Phys. Lett. **88**, 251106 (2006).
12. S. Furumi and Y. Sakka, Adv. Mater. **18**, 775 (2006).
13. M. Mitov and N. Dessaud, Nat. Mater. **5**, 361 (2006).
14. M. P. Groenewege, Mol. Phys. **5**, 541 (1962).
15. W. F. Brown, Jr., S. Shtrieman and D. Treves, J. Appl. Phys. **34**, 1233 (1963).
16. D. L. Portigal and E. Burstein, J. Phys. Chem. Solids **32**, 603 (1971).
17. N. B. Baranova, Y. V. Bogdanov, and B. Y. Zel'Dovich, Opt. Commun. **22**, 243 (1977).
18. N. B. Baranova and B. Y. Zel'Dovich, Mol. Phys. **38**, 1085 (1979).
19. G. Wagnière and A. Meier, Chem. Phys. Lett. **93**, 78 (1982).
20. L. D. Barron and J. Vrbancich, Mol. Phys. **51**, 715 (1984).
21. G. L. J. A. Rikken and E. Raupach, Nature **405**, 932 (2000).
22. A. Christofi and N. Stefanou, Phys. Rev. B **97**, 125129 (2018).
23. V. Doormann, J. P. Krumme, and H. Lenz, J. Appl. Phys. **68**, 3544 (1990).
24. S. M. Drezdzon and T. Yoshie, Opt. Express **17**, 9276 (2009).
25. K. Fang, Z. Yu, V. Liu, and S. Fan, Opt. Lett. **36**, 4254 (2011).
26. Y. Tajitsu, R. Hosoya, T. Maruyama, M. Aoki, Y. Shikinami, M. Date, and E. Fukada, J. Mater. Sci. Lett. **18**, 1785 (1999).
27. T. Inui, Y. Tanabe, and Y. Onodera, *Group Theory and Its Applications in Physics* (Springer, 1990).
28. P. Varytis, P. A. Pantazopoulos, and N. Stefanou, Phys. Rev. B **93**, 214423 (2016).
29. M. Kim, J. An, K. S. Kim, M. Choi, M. Humar, S. J. J. Kwok, T. Dai, and S. H. Yun, Biomed. Opt. Express **7**, 4220 (2016).
30. M. H. Hutchinson, J. R. Dorgan, D. M. Knauss, and S. B. Hait, J. Polym. Environ. **14**, 119 (2006).
31. G. L. J. A. Rikken and E. Raupach, Phys. Rev. E **58**, 5081 (1998).
32. A. Christofi and N. Stefanou, Opt. Lett. **38**, 4629 (2013).
33. V. Yannopapas and A. G. Vanakaras, ACS Photonics **2**, 1030 (2015).